Projection of Pixel-based Rice Yields by Linking Geostationary Satellite Imagery and a Crop Model in Northeast Asia

Seungtaek Jeong (1*), Jonghan Ko (1), Jong-min Yeom (2)

[1] Chonnam National University, 77 Yongbong-ro, Buk-gu, Gwangju 61186, Korea
[2] Korea Aerospace Research Institute, 169-84 Gwahak-ro, Yuseong-gu, Daejeon 34133, Korea
Email: jst5000@gmail.com; jonghan.ko@jnu.ac.kr; yeomjm@kari.re.kr

KEY WORDS: Crop model, COMS, GRAMI, rice yield, satellite

ABSTRACT: An approach of linking satellite imagery and a crop model can allow reproducing geospatial variation in crop productivity efficiently and conveniently. This methodology could be a useful means of responding to ever-increasing food crop demand and managing its production. This study aims to simulate rice yields with geographical changes based on the Communication, Ocean, and Meteorological Satellite (COMS) data incorporated into the GRAMI-rice model in most continental areas of Northeast Asia of interest from 2011 to 2014. The COMS consists of two imager payloads, the Geostationary Ocean Color Imager (GOCI) and the Meteorology Imager (MI), from which surface reflectance and solar radiation were obtained to use as input variables of the model. The GOCI imagery has an advantage of reducing a cloud effect in comparison with any other images from polar orbit satellites, owing to being obtained through frequent observations, i.e., eight times a day. We also used Local Data Assimilation and Prediction System (LDAPS) and Shuttle Radar Topography Mission (STRM) Digital Elevation Model (DEM) data to acquire air temperature and geographic information such as an elevation and a surface slope. Before simulating rice yields, we first performed a classification of paddy fields and estimation of transplanting dates using time-series of spectral indices and geographical characteristics of rice cultivation. After that, the model evaluation that can reflect regional characteristics of the rice cultivars and farming practices was performed and compared with county-level statistical yield data of the study areas. The overall accuracy and the Kappa coefficient of the classified paddy fields were 78.8 % and 51.2 %, respectively. The root mean square error (RMSE), Nash-Sutcliffe efficiencies (NSE), and *p*-values of two-sample *t*-tests between observed and simulate rice yields ranged from 0.673 to 0.767 t ha^{-1}, 0.108 to 0.478, and 0.130 to 0.894, respectively.

1. Introduction

Rice (*Oryza sativa*) is one of the major staple crops, which more than half of the world's population consumes. Especially, over 90 % of the world's rice has been cultivated in Asia (MacLean *et al*., 2013). Monitoring of rice production for future food security is an important activity in the current situation in which the population is steadily growing. Satellite imagery has been employed due to its convenience and efficiency to monitor rice productivity in a broad area (Jeong *et al*., 2018). The empirical crop model is one of the earliest, easily, and more practical modeling approaches, but it is only available in limited areas and environments where it was developed (Doraiswamy and Cook, 1995; Reeves *et al*., 2005). Meanwhile, using process-based crop models can provide opportunity to obtain continuous information on crop growth and development based on crop biophysical processes (Ahuja *et al*., 2000; Hodson and White, 2010). However, since a considerable number of inputs is required, spatial monitoring for a broad area is challenging unless the various spatial inputs required by the crop model are efficiently comprised. In this study, we simulated rice yields by linking the Geostationary Ocean Color Imager (GOCI) and process-based GRAMI-rice model in Northeast Asia from 2011 to 2014. The sub-objectives of the study are to (1) detect the spatial distribution of rice fields, (2) perform regional parametrization of the GRAMI model, and (3) validate the classified paddy fields and simulated rice yields.

2. Data and methods

2.1 Study area

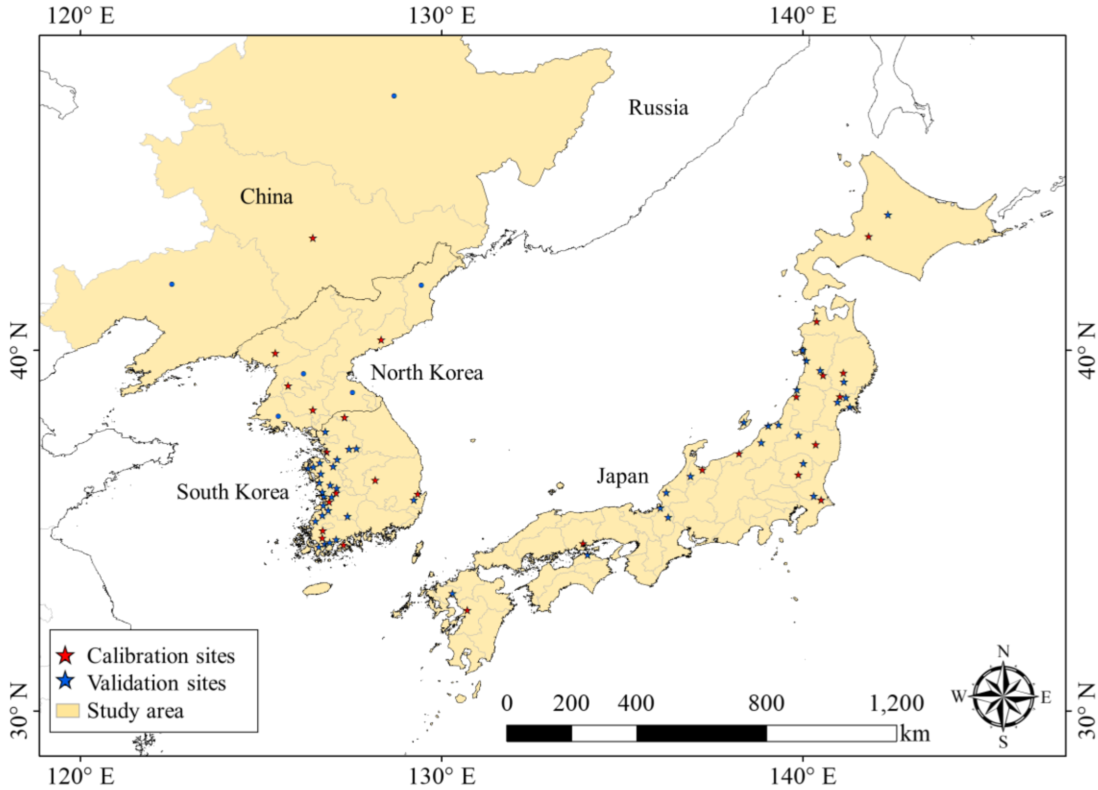

Figure 1. Study area for the simulation and spatial projection of rice yield. The red and blue stars indicate locations for calibration and validation, respectively, of the crop model applied in counties (provinces in the case of North Korea and China) where rice is primarily cultivated.

The study area was limited to the GOCI entire disk area covering all of the nations of South and North Korea, Japan, and the northeastern (NE) parts of China (Figure 1). The NE China is a granary zone that mainly includes important plains such as Sanjiang, Songnen, and Liaohe (Dong *et al.*, 2016). The study regions vary from a cold temperate monsoon climate in the NE China to a subtropical monsoon climate in southern Japan (Peel *et al.*, 2007).

2.2 Data

COMS

The Communication, Ocean, and Meteorological Satellite (COMS) was launched on June 27, 2010 by the Korea Aerospace Research Institute. In this study, vegetation index and solar insolation data used as input variables to the GRAMI model were obtained from the GOCI and Meterological Imager (MI) sensors of COMS, respectively. Surface reflectance from GOCI in eight multi-spectral bands ranges from visible to near-infrared wavelengths with a spatial resolution of 500 m, obtained at every hour from 09:00 to 16:00 KST. The reliable reflectance was computed according to an atmospheric correction process using the second simulation of the satellite signal in the solar spectrum (6S) model and a semi-empirical bidirectional reflectance distribution function to correct the surface anisotropy effects. Daily solar insolation with a spatial resolution of 1 km was acquired from the COMS MI data using the Kawamura physical model (Kawamura *et al.*, 1998) modified by Yeom *et al.*, 2016.

MODIS
MODIS MYD09A1 surface reflectance data from the Aqua satellite (https://ladsweb.modaps.eosdis.nasa.gov/) were used together with the GOCI data to detect the spatial distribution of paddy fields. Adequate reflectance data with a spatial resolution of 500 m were selected about at an eight day interval considering the effects of atmospheric water vapor and clouds. Simple linear interpolation was adopted to reduce a cloud contamination effect during the crop growing season utilizing the cloud information data from quality control flags, which is attributed to the typical monsoonal cloudy conditions.

RDAPS and SRTM DEM
The spatial temperature data with a spatial resolution of 12 km were obtained from the Regional Data Assimilation and Prediction System (RDAPS) based on the fifth-generation Mesoscale Model (Grell *et al*., 1994) provided by the Korea Meteorological Administration. Digital elevation map (DEM) data were obtained from the highest-resolution digital topographic database of the Earth, which was generated by the Shuttle Radar Topography Mission (SRTM) model of United States National Aeronautics and Space Administration (NASA). The database provides a world DEM with a spatial resolution of 90 m based on Interferometric Synthetic Aperture Radar data (Rabus *et al*., 2003). In this study, surface elevation and slope were calculated from the DEM data.

Land cover maps
We obtained high-spatial-resolution land cover maps of South Korea and Japan produced in 2013 and 2014, respectively. These maps were used to determine the threshold values for detection of paddy fields and validate the classified paddy fields. The maps were provided by the Environmental Geographic Information Service (EGIS) of the Korea Ministry of Environment (KME) (https://egis.me.go.kr) and by the Earth Observation Research Center (EORC) of the Japan Aerospace Exploration Agency (JAXA) (https://www.eorc.jaxa.jp). In the case of NE China and North Korea, it was assumed to have the same characteristics as South Korea and Japan because of the inaccessibility of official national land cover maps.

2.3 Methods

Rice classification
Unlike other staple crops, paddy rice has a unique characteristic of growing on wetlands. On the basis of this characteristic, Xiao *et al*. (2005) proposed a simple condition to detect the irrigation water signal using the interrelationship of normalized difference vegetation index (NDVI), land surface water index (LSWI), and the threshold (T) of the LSWI, which is LSWI + $T \geq$ NDVI. In addition, several thresholds related to the characteristics of rice cultivation were used as follows: an altitude and a surface slope, the maximum and minimum NDVIs, and an NDVI increase rate with a scale factor of 1,000, which was calculated from values between the minimum and maximum NDVIs.

GRAMI-rice model
GRAMI was initially designed to receive remote sensing data as an input variable to obtain a mathematical agreement between simulation and measurement based on the “within-season” calibration procedure (Maas, 1993). The model includes four main crop growth processes: (1) calculation of growing degree days (GDD) using daily mean temperatures and a base temperature of rice, (2) determination of the absorption of daily incident radiation energy by leaves, (3) computing new dry mass produced by the rice canopy, and (4) determination of LAI partitioning from a new dry mass. More details can be referenced from Ko *et al*. (2015) and Jeong *et al*. (2018).

3. Results and discussion

3.1 Classification of paddy fields

The threshold values were determined based on compositing the training dataset (75,000 paddy and 150,000 non-paddy pixels), as follows: altitude = 800 m; surface slope = 7°; maximum and minimum NDVIs of 0.43 and 0.42; an NDVI increase rate of 2.0; and a T value of 0.17. Following application of these thresholds to the validation dataset (25,000 paddy and 50,000 non-paddy pixels), the overall accuracy and the Kappa coefficient of detected paddy fields were 78.8 % and 51.2 %, respectively (Table 1). The user's accuracy values for the paddy and non-paddy fields were 69.7 % and 82.7 %, having the producer's accuracy values as 64.1 % and 86.1 %, respectively (Table 1).

Table 1. Error matrix to validate the spatial distribution of classified paddy fields from Geostationary Ocean Color Imager (GOCI) and Moderated Resolution Imaging Spectroradiometer (MODIS) data for South Korea in 2013 and Japan in 2014.

		Reference			User's accuracy (%)
		Paddy	Non-paddy	Total	
Classification	Paddy	16,021	6,953	22,974	69.7
	Non-paddy	8,979	43,047	52,026	82.7
	Total	25,000	50,000	75,000	
Producer's accuracy (%)		64.1	86.1		
Overall accuracy = 78.8%, Kappa coefficient = 51.2%					

The classification approach used in this study has been widely applied to detect the distribution of paddy fields, irrigated areas, or flooding areas based on optical satellite imagery (Xiao *et al*, 2005; Peng *et al*., 2011). The concept is a simple and clear logic that reflects the spectral time series for characteristics of the paddy fields. The study results have shown reliable analytical indices, meaning that the methodology is highly expandable. Meanwhile, the T value of the LSWI used to increase the LSWI's sensitivity to irrigation water can vary depending on the characteristics of the land covers. This variability can lead to potential errors in case of using other satellite imagery or when targeting different regions. Therefore, it is necessary to determine the T value carefully. We consider that if variable T values can be applied according to the characteristics of land covers, more reliable classification can be obtained (Jeong *et al*., 2012).

3.2 Simulation of rice yields

Simulated rice yields using GOCI images and the GRAMI-rice model were compared to the reported regional rice yields. The comparison analysis results showed a significant agreement range in most study areas. The root mean square error (RMSE), Nash-Sutcliffe efficiency (NSE), and p values ranged from 0.620 to 0.676 t ha^{-1}, 0.108 to 0.660, and 0.130 to 0.953, respectively (Table 2 and Figure 2). In the spatial distribution of the simulated rice yields (Figure 3), the interannual variation in North Korea was found to be higher than that in the other countries. We consider that this tendency is attributable to the poor irrigation infrastructures in the country. Rice yields were similar between South Korea and NE China, showing somewhat lower yields in Japan. It is considered that this difference is related with rice varieties and factors to focus on rice cultivation. Rice in South Korea and China tends to be cultivated to increase yield through an intensive management practice applying more nitrogen fertilizers than that in Japan where rice cultivation is practiced with a focus on quality rather than yield (Ko *et al*., 2014).

Table 2. Root mean square errors (RMSE), Nash-Sutcliffe efficiencies (NSE), and *p* values of two-sample *t*-tests between observed and simulated rice yields in 54 counties (or provinces) of interest in Northeast Asia from 2011 to 2014.

Year	Observation	Simulation	RMSE	NSE	*t* test
-	--------------------	t ha^{-1}	--------------------	-	--- *p* ---
2011	6.02	6.10	0.673	0.478	0.683
2012	5.98	5.82	0.684	0.286	0.314
2013	6.24	6.27	0.685	0.353	0.894
2014	6.45	6.16	0.767	0.108	0.130

We consider that our results are comparable with those of earlier studies conducted using the GRAMI model (Jeong *et al*., 2018; Yeom *et al*., 2018) even though this study was performed in a wider area. Also, similar reliable results were obtained from other previous studies that employed different crop models to simulate rice yields based on coarse spatial resolution images such as MODIS (Tomar *et al*., 2014; Son *et al*., 2014). While the GOCI is limited to northeast Asia in the study area, it allows to obtain satellite images with a stable time series. When other satellite images are applicable to simulate more reliable rice yield using the GRAMI model for a wider area, much more efforts are needed in image processing such as atmospheric correction or gap-filling due to mainly cloud contamination since the model is dependent on remote sensing data. However, the GRAMI model can be applied to any areas of interest on the Earth's surface depending on the availability of reliable satellite images.

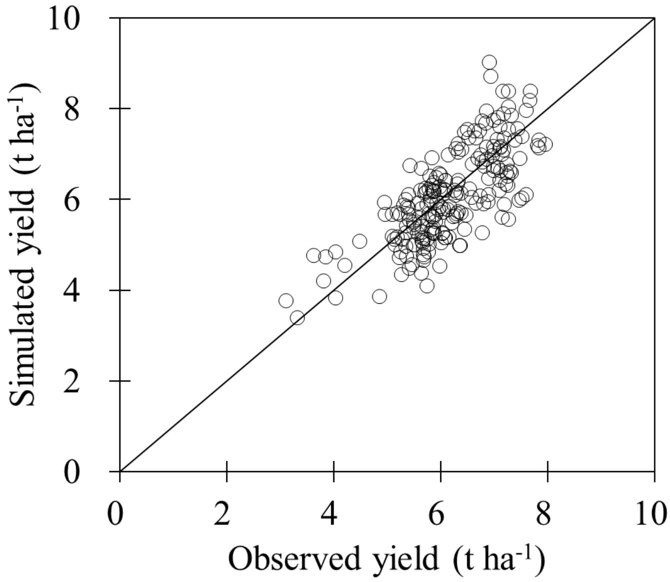

Figure 2. Comparisons of observed and simulated rice yields (t ha^{-1}) for 54 validation counties (or provinces) in Northeast Asia from 2011 to 2014. The bold line is 1:1 lines.

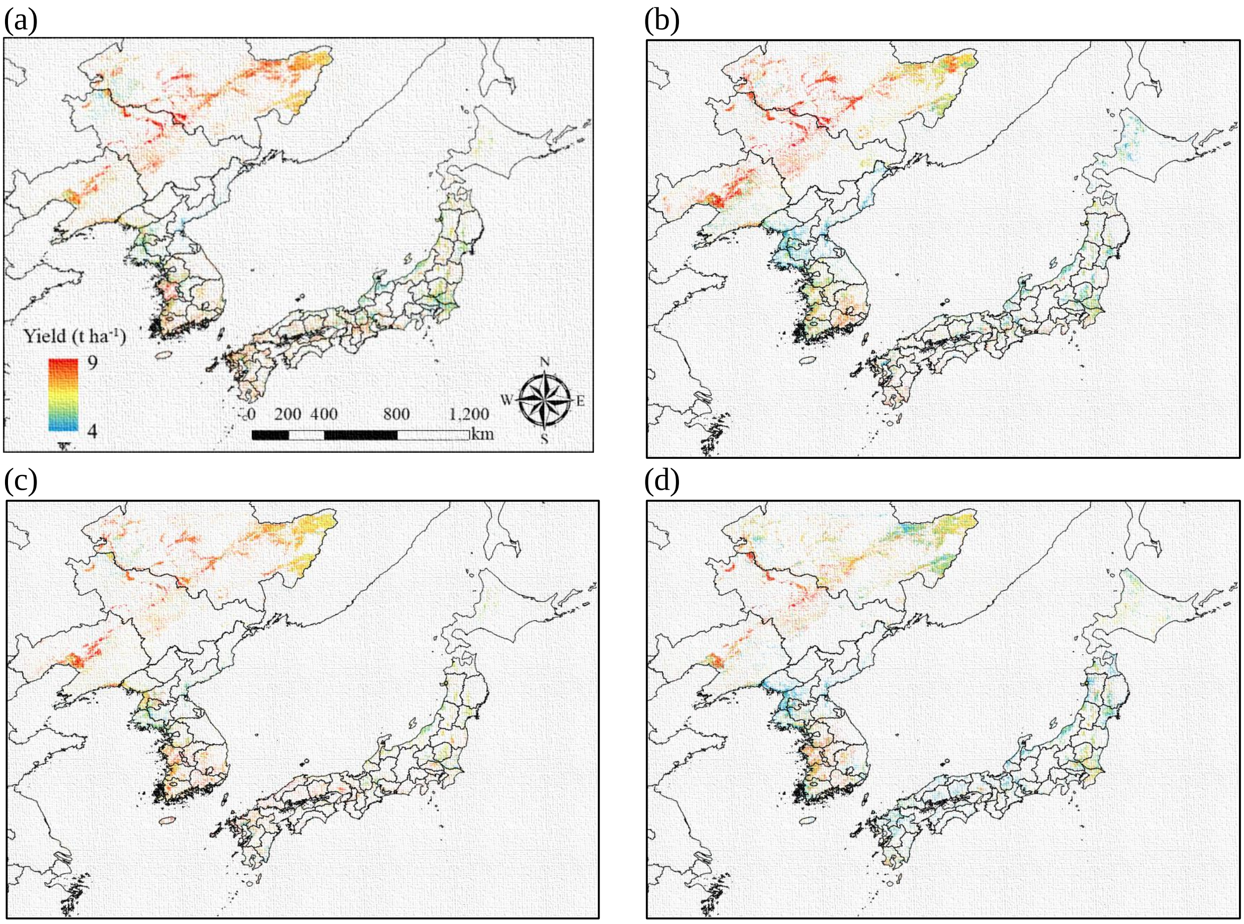

Figure 3. Spatial distribution of simulated rice yields in Northeast Asia from 2011 to 2014 (a–d, respectively) based on Communication, Ocean, and Meteorology Satellite (COMS) images and the GRAMI-rice model.

4. Conclusion

In this study, rice yields were successfully simulated using GOCI images and the GRAMI-rice model in North and South Korea, Japan, and NE China from 2011 to 2014. The overall accuracy between simulation and observation was in a significant agreement range in a county (or province) scale. Our results showed the possibility of obtaining reliable crop yield information by combining the process-based crop model and geostationary satellite images. Although we only simulated just rice yield in this study, continuous and diverse crop growth information can be obtained spatially due to the process-based crop model feature. We believe that the whole methodologies employed in this study may help to manage staple food crop production through understanding the current circumstances of crop productivity.

5. References

Ahuja, L.R., Rojas, K.W., Hanson, J.D., Shaffer, M.J., Ma, L., 2000. Root zone water quality model: modeling management effects on water quality and crop production. Water Resources Publications, LLC, Highland Ranch, CO, USA.

Dong, J., Xiao, X., Menarguez, M.A., Zhang, G., Qin, Y., Thau, D., Biradar, C., Moore, B., 2016. Mapping paddy rice planting area in northeastern Asia with Landsat 8 images, phenology-based algorithm and Google Earth Engine. Remote Sensing of Environment 185, 142-154.

Doraiswamy, P.C., Cook, P.W., 1995. Spring Wheat Yield Assessment Using NOAA AVHRR Data. Canadian Journal of Remote Sensing 21, 43-51.

Grell, G.A., Dudhia, J., Stauffer, D.R., 1994. A description of the fifth-generation Penn State/NCAR mesoscale model (MM5).

Hodson, D., White, J., 2010. GIS and crop simulation modelling applications in climate change research, in: Reynolds, M.P. (Ed.), Climate Change and Crop Production. CABI, Cambridge, MA, 245-262.

Jeong, S., Kang, S., Jang, K., Lee, H., Hong, S., Ko, D., 2012. Development of Variable Threshold Models for detection of irrigated paddy rice fields and irrigation timing in heterogeneous land cover. Agricultural Water Management 115, 83-91.

Jeong, S., Ko, J., Yeom, J.-M., 2018. Nationwide Projection of Rice Yield Using a Crop Model Integrated with Geostationary Satellite Imagery: A Case Study in South Korea. Remote Sensing 10, 1665.

Ko, J. K., Park, H. K., Kang, S. G., Kato, H., Ishii, T., Nemoto, H., Sakai M, Satou K., Ikuo, A., Kim, B.-K., 2014. Comparison of rice grain yield and quality of different maturity groups by cultivating in Korea and Japan. Journal of the Korean Society of International Agricultue 26, 353-359.

Kawamura, H., Tanahashi, S., Takahashi, T., 1998. Estimation of insolation over the Pacific Ocean off the Sanriku coast. Journal of Oceanography 54, 457-464.

Maas, S.J., 1993. Within-season calibration of modeled wheat growth using remote sensing and field sampling. Agronomy Journal 85, 669-672.

Peel, M.C., Finlayson, B.L., McMahon, T.A., 2007. Updated world map of the K¨oppen-Geiger climate classification. Hydrology Earth System Science 11, 1633-1644.

Peng, D., Huete, A.R., Huang, J., Wang, F., Sun, H., 2011. Detection and estimation of mixed paddy rice cropping patterns with MODIS data. International Journal of Applied Earth Observation and Geoinformation 13, 13-23.

Rabus, B., Eineder, M., Roth, A., Bamler, R., 2003. The shuttle radar topography mission - a new class of digital elevation models acquired by spaceborne radar. ISPRS journal of photogrammetry and remote sensing 57, 241-262.

Reeves, M.C., Zhao, M., Running, S.W., 2005. Usefulness and limits of MODIS GPP for estimating wheat yield. International Journal of Remote Sensing 26, 1403-1421.

Son, N. T., Chen, C. F., Chen, C. R., Minh, V. Q., Trung, N. H., 2014. A comparative analysis of multitemporal MODIS EVI and NDVI data for large-scale rice yield estimation. Agricultural and Forest Meteorology 197, 52-64.

Tomar, V., Mandal, V.P., Srivastava, P., Patairiya, S., Singh, K., Ravisankar, N., Subash, N., Kumar, P., 2014. Rice equivalent crop yield assessment using MODIS sensors' based MOD13A1-NDVI data. IEEE Sensors Journal, 14, 3599-3605.

Xiao, X., Boles, S., Liu, J., Zhuang, D., Frolking, S., Li, C., Salas, W., Moore, B., 2005. Mapping paddy rice agriculture in southern China using multi-temporal MODIS images. Remote Sensing of Environment 95, 480-492.

Yeom, J.-M., Jeong, S., Jeong, G., Ng, C.T., Deo, R.C., Ko, J., 2018. Monitoring paddy productivity in North Korea employing geostationary satellite images integrated with GRAMI-rice model. Scientific reports 8, 16121.

Yeom, J.-M., Seo, Y.-K., Kim, D.-S., Han, K.-S., 2016. Solar Radiation Received by Slopes Using COMS Imagery, a Physically Based Radiation Model, and GLOBE. Journal of Sensors 2016, 1-15.

MacLean, J.L., Dawe, D.C., Hardy, B., Hettel, G.P., 2013. Rice Almanac: sourcebook for the most important economic activity on Earth Fourth Edition Ed. Global Rice Science Partnership, International Rice Research Institute, Metro Manila, Philippines.